Applied Physics A (2023) 129:564
https://doi.org/10.1007/s00339-023-06832-6

Applied Physics A
Materials Science & Processing

An investigation into green synthesis of Ru template gold nanoparticles and the in vitro photothermal effect on the MCF-7 human breast cancer cell line

Leili Shabani[1] · Seyed Reza Kasaee[2] · Shreeshivadasan Chelliapan[3] · Milad Abbasi[1] · Hossein Khajehzadeh[1] · Fatemeh Sadat Dehghani[1] · Tahereh Firuzyar[4] · Mostafa Shafiee[1] · Ali Mohammad Amani[1] · Sareh Mosleh-Shirazi[5] · Ahmad Vaez[6] · Hesam Kamyab[7,8]

Received: 24 December 2022 / Accepted: 18 June 2023 / Published online: 19 July 2023

Abstract

In recent years, laser photothermal therapy of cancers, as a new adjuvant treatment, has attracted a lot of attention. Nanoparticles have been applied to increase the effect of plasmonic photothermal therapy (PPTT) with decreasing side effects. Plasmonic photothermal therapy using gold nanoparticles (Au NPs) has been employed as a novel approach for PPTT. In this research, Au NPs were green synthesized by utilizing Rutin extract as a stabilizing and reducing agent. Afterward, structural and physical characteristics were evaluated by the use of transmission electron microscopy (TEM), and visible–ultraviolet spectrophotometer (UV–Vis). Biocompatibility and cytotoxicity of nanoparticles are tested using the MTT method. The therapeutic effect of this nanoparticle on breast cancer cells was investigated in vitro using a laser with a power of 500 mW and a wavelength of 532 nm. Microscopic images revealed that the synthesized Au NPs had the mean size of 40 nm and a roughly spherical form. The results indicate the selective and effective anticancer function of Ru-Au NPs, in addition to low cytotoxicity and better biocompatibility for normal cells. Also, the findings demonstrate the significant efficacy of Ru-Au NPs coupled with laser radiation (150 J/cm^2 of laser energy for 300 s) in the treatment of breast cancer MCF-7 cells. As a result of the study, an ecoenvironmental nanoplatform for PPTT against MCF-7 human breast cancer cell line with excellent anticancer function and acceptable biocompatibility has been developed.

Keywords Gold nanoparticles · Plasmonic photothermal therapy · Laser absorption · Breast cancer treatment

✉ Ali Mohammad Amani
amani_a@sums.ac.ir

✉ Sareh Mosleh-Shirazi
mosleh@sutech.ac.ir

✉ Ahmad Vaez
ahmadvaez@yahoo.com

✉ Hesam Kamyab
hesam_kamyab@yahoo.com

[1] Department of Medical Nanotechnology, School of Advanced Medical Sciences and Technologies, Shiraz University of Medical Sciences, Shiraz, Iran

[2] Shiraz Endocrinology and Metabolism Research Center, Shiraz University of Medical Sciences, Shiraz, Iran

[3] Engineering Department, Razak Faculty of Technology and Informatics, Universiti Teknologi Malaysia, Jalan Sultan Yahya Petra, 54100 Kuala Lumpur, Malaysia

[4] Department of Nuclear Medicine, School of Medicine, Shiraz University of Medical Sciences, Shiraz, Iran

[5] Department of Materials Science and Engineering, Shiraz University of Technology, Shiraz, Iran

[6] Department of Tissue Engineering and Applied Cell Sciences, School of Advanced Medical Sciences and Technologies, Shiraz University of Medical Sciences, Shiraz, Iran

[7] Department of Biomaterials, Saveetha Dental College and Hospital, Saveetha Institute of Medical and Technical Sciences, Chennai 600 077, India

[8] Malaysia-Japan International Institute of Technology (MJIIT), Universiti Teknologi Malaysia, Jalan Sultan Yahya Petra, 54100 Kuala Lumpur, Malaysia

1 Introduction

Hyperthermia is defined as an effective and new adjuvant treatment technique that elevates tissue temperature by utilizing near-infrared (NIR) light for a definite duration of time to destruct cancer cells [1]. Traditional treatment of cancers by applying laser photodynamic therapy (PDT) has some limitations, such as insufficient penetration's depth and damage to surrounding normal tissue [2].

Recently, nanoparticle mediated photothermal therapy (PTT) has attracted significant attention for its ability to increment the effect of PTT and decline side effects and there have been great advances in this field in the last decade [3–5]. Some ferromagnetic nanoparticles applied for hyperthermic PTT include ferrite and iron oxide nanoparticles are typically stimulated in the presence of alternating magnetic fields (AMFs) with the limitation of fluctuation in magnetization fields [6].

Plasmonic photothermal therapy (PPTT) is a novel approach of PTT, that metallic nanoparticles are exposed to laser irradiation near their plasmon-resonant absorption band to deactivate and activate electrons. Gold nanoparticles have specific surface plasmon resonance characteristics with excellent optical properties that could be applied for diagnosis and plasmonic PTT of cancers [3, 4, 7–10]. According to the unique physico-chemical and biological characteristics of gold nanoparticles (Au NPs), different designed forms of Au NPs such as nanosphere, nanorod, and nanoshell have been produced for biomedical applications especially as plasmonic resonance agents in PTT [11–18]. In 2003, Pitsillides et al. conducted a selective photothermal treatment of T cell lymphoma with targeted gold nanoparticles for the first time [19]. In another study, colloidal Au linked to adenoviral vectors has been applied for selective cancer targeting and induces hyperthermia through utilizing near-infrared (NIR) laser light [20].

In recent years, the green synthesis of gold nanoparticles from various biological sources, including plant extracts (tea phytochemicals, garlic extract, soybeans,…) or microorganisms, has opened a new window to improve the biological and physical properties of gold NPs for biomedical applications [21–24]. Variations in reaction conditions of green synthesis method could result in nanoparticles with different dimensions or structures, which exhibit excellent durability as well as cytocompatibility.

Ruta graveolens L. (Garden Rue) is the Rutaceae family cultivated in different parts of the world as a medicinal herb [25]. Rutin (Ru) is the superlative abundant flavonoid glycoside in *R. graveolens* L. that has been considered for the gold NPs' synthesis as a natural precursor [26–28]. Ru flavonoidal skeleton has significant pharmacological specialties such as antioxidant, antibacterial, anticancer, anti-inflammatory, anti-hyperlipidemia, anti-hyperglycemia, myocardial protecting, hepatoprotective activities, antiulcer, and analgesic [29–31]. Previous studies have revealed the anti-arthritic, anti-inflammatory and antiproliferative actions of Ru-Au NPs [26–28]; nevertheless, there are no previous report to investigate the photothermal effect of Ru-Au NPs on the MCF-7 human breast cancer cell line.

In this study, Au nanoparticles (NPs) have been green synthesized using Rutin (Ru) extract as a reductant and stabilizing agent. Physiochemical characteristics and anticancer function of Ru-Au nanoparticles (NPs) against MCF-7 breast cancer cells either alone or in the presence of laser PTT have been discussed; also, the safety of Ru-Au NPs for normal fibroblasts cells was investigated.

2 Materials and methods

2.1 Materials

For the synthesis of Au NPs, gold chloride with the scientific name of hydrogen tetrachloroaurate ($HAuCl_4$) with a molecular mass of 785.339 g/mol was prepared by Merck Company. A T75 flask containing the MCF-7 cell lines was provided from the Shiraz University of Medical Sciences' research center. All cell culture media, including RPMI, DMEM, antibiotics (penicillin/streptomycin), FBS, PBS, DMSO, and trypsin IX were purchased from Sigma. MTT (3-(4,5 dimethylthiazole-2-yl)-2,5-diphenyl tetrazolium) was purchased from Sigma-Aldrich, USA. The 96 plates and 3.5 cm microplate were provided by MAXWELL Malaysia.

2.2 Synthesis of gold nanoparticles (Ru-Au NPs)

R. graveolens L. leaves were collected, washed with distilled water, and then dried at ambient temperature in shade. 3 L methanol (80%) with dried milled of *R. graveolens* powders (300 g) ultra-sonicated for 1 h. The solution was filtered through Whatman filter paper, dissolved in 500 mL of distilled water, and then defatted with 500 mL of *n*-hexane. The aqueous layer was fractionated with chloroform to remove the semipolar compounds. Subsequently, the water-soluble part was kept for 72 h in the refrigerator to separate the yellowish precipitate from the solution. The obtained precipitate was washed sequentially with methanol, chloroform, ethyl acetate, and acetone and dried to attain Rutin powder (1.376 g).

Rutin ($C_{27}H_{30}O_{16}$) (Fig. S1) was used as a reducing/ capping agent to biosynthesize Au NPs. To synthesize these nanoparticles, varying concentrations of Ru (5, 10, and 15 mM) were added dropwise to a constant concentration of gold salt (10 mM) with constant stirring at ambient temperature.

Furthermore, the color of the mixture changed from light yellow to wine red after 30 min. The metal ions' reduction was continuously monitored by visual inspection and measured with a UV–visible spectrometer at the wavelength of 300–800 nm, and the strongest color shift was performed at the optimum concentration of Ru (10 mM) (Fig. S2).

2.3 Characterization of nanoparticles

The transmission electron microscope [TEM, ZEISS 10A conventional TEM model, Carl Zeiss-EM10C-100 kV (Germany)] was employed to evaluate the size and morphology of Ru-Au NPs. TEM samples were provided with well-scattered NPs drops on the 300-mesh carbon-coated copper grid [32]. The FT-IR spectroscopy analyses were performed using a (Nicolet IS10, Thermo Scientific, USA), at 4000–400 cm^{-1}. The absorption peak of Ru-Au NPs was obtained by a UV–vis spectrophotometer (Varian, model; Carry 100) at 200–800 nm.

2.4 Cytotoxicity assessment of Ru-Au NPs

The in vitro cytotoxicity of the Ru-Au NPs was investigated against MCF-7 breast cancer cell lines by the MTT colorimetric assay. The cell lines and culture medium served as positive and negative controls in this assay, respectively. The result is determined by the reduction of MTT to purple-colored formazan crystals through the mitochondrial dehydrogenases activity in viable cells.

The optical absorption (OD) of formazan products is analyzed spectrophotometrically (570 nm) after dissolution in DMSO. Furthermore, the spectra of Ru-Au NPs-untreated and treated cells give an estimate of the extent of cytotoxicity. A certain cell number (10,000 cells per well) were seeded in the 96-well microplate and incubated in a humidified atmosphere of 5% CO_2 and 95% air at 37 °C to obtain 70–90% confluence. Subsequently, different concentrations of Ru-Au NPs were added to each well. The medium was eliminated from each well and washed two times for 2–3 min with the phosphate-buffered saline (PBS) solution after 24, 48, and 72 h of incubation. The MTT stock solution (25 µl) was transferred to each well and subsequently incubated in a humidified atmosphere of 95% air and 5% CO_2 for 4 h at 37 °C. Furthermore, the OD of the solution was read by an Elisa plate reader (Model 50, Bio-Rad Corp, Hercules, and CA) after dissolution in DMSO at a wavelength of 570 nm. All experiments were examined in triplicate.

2.5 Photothermal treatment of MCF-7 breast cancer cells

The PL532 laser, with a wavelength of 532 nm and a maximum energy of 500 mW, from the Osram Company, made in Germany, was performed to deliver laser dose irradiation. Furthermore, the space between the laser probe and the cell plate was 2 cm and the area of the laser spot was 1 cm^2. Time of the laser exposure was 300 s. The laser beam was immediately irradiated to the cell plate.

In accordance with the cytotoxicity assessment section, 96-well cell cultures for four groups (G1–G4) were prepared. Furthermore, the groups G1 to G3 received 150 J/cm^2 of laser energy, 30 µg/mL of Ru-Au NPs + 150 J/cm^2 laser energy, as well as 30 µg/mL of Ru-Au NPs, respectively. Group G4 was considered as the control group and did not get any laser energy or Ru-Au NPs.

For photothermal treatment in group G2, MCF-7 cells were seeded and treated with 30 µg/mL Ru-Au NPs, as described in the above section. The treated cells were incubated at 37 °C for 3 h, followed by irradiation with laser energy of 150 J/cm^2 for 300 s. Group G1 was only irradiated with laser energy of 150 J/cm^2 for 300 s and also, group G3 was only treated with 30 µg/mL Ru-Au NPs as described in the above section. Finally, the cells of four groups were incubated at 37 °C for another 24, 48, and 72 h, and the number of MCF-7 cells after treatment and their viability were measured by Inverted Stage Microscope and MTT assay, respectively. All experiments were carried out in triplicate.

2.6 Statistical analysis

Statistical Package for Social Sciences (SPSS) software (version 20.0, developed by SPSS Inc. in Chicago, Illinois, USA) was performed to statistically analyze data after gathering and recording all information. Comparisons between treated groups and controls were evaluated by one-way ANOVA combined with Bonferroni post-analysis. A p value equal to or less than 0.05 was considered statistically significant for differences between the mentioned groups.

3 Results and discussion

3.1 Synthesis and characterization of Ru-Au nanoparticles

Ru-Au NPs were synthesized according to the green chemistry method from Ru extract. The pH of the gold solution with the Ru extract was changed to 7.0 to improve the bioavailability of the substances contained in the extract. Furthermore, the pH change aids the triggering of phytochemical substances, allowing for the donation of electrons to the metallic material and the reduction of Au^{3+} to Au. The biosynthesis pathway creates nanostructures of varying morphology and dimensions [33–35].

The UV–Vis absorption of Rutin extract and Ru-Au NPs were investigated in the range of 200–700 nm (Fig. 1). The

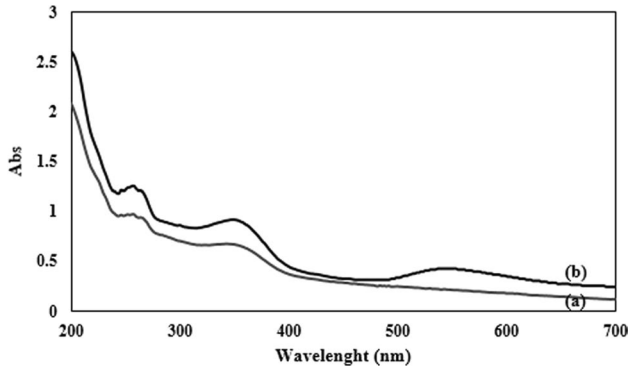

Fig. 1 UV–Vis spectra of **a** Ru extract and **b** Ru-Au NPs

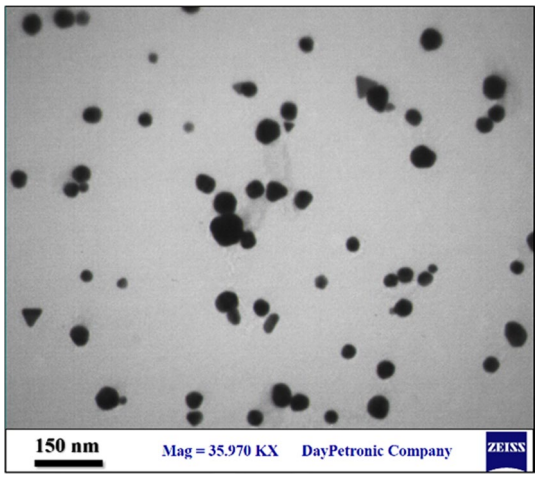

Fig. 2 TEM micrographs of Ru-Au nanoparticles

Au NPs possess a peculiar optical property known as localized surface plasmon resonance (LSPR) [36]. In nanoscale dimensions, this band can be located on the surface of some metallic materials. The Ru-Au NPs have a maximum absorption at 520–540 nm that relates directly to the formation of spherical Au NPs. Based on the literature report, the single plasmon band about 527 nm corresponds to a spherical gold particle with a diameter of approximately 20 nm [37]. Rutin extraction has two absorption peaks at 262 and 358 nm (Fig. 1a). The SPR of Ru-Au NPs displays a blue shift in these peaks compared to Ru extracts due to the interaction between gold and rutin molecules (Fig. 1b). Nevertheless, the plasmonic band of Ru-Au NPs is broad, and any physical characteristics of shape or size can be determined only based on the plasmonic band position. At lower Ru concentrations (5 mM), the SPR peak is broad with long wavelength absorption, which reveals anisotropy in the Au NPs' shape. Whenever the leaf concentration increments, the band shifts towards a lower wavelength (Fig. S2). Eventually, at 536 nm, a sharper absorption peak, is determined as a characteristic of spherical particles in 10 mM Rutin [38, 39].

The average crystallite size and morphology of Ru-Au NPs were determined by TEM imaging. The TEM images of Ru-Au NPs (Fig. 2) suggest a narrow distribution of particle size with diameter distribution peaks around 40 nm and spherical morphology. The smaller nanostructures had spherical morphology, while the larger ones had a variety of geometric patterns, including triangles, pentagons, and rods. Philip et al. [40], Smitha et al. [41], and Gosh et al. [42] observed that nanostructures with distinct geometric shapes were bigger than those with spherical structures owing to reduced concentration levels of the effective organic compounds necessary for stabilization and capping, resulting in sizeable anisotropic nanostructures.

FTIR spectroscopy is considered a useful tool to evaluate a variety of functional groups and the alterations in them after chemical reactions. The FTIR spectra of Au NPs showed a narrower absorption band near 3400 cm^{-1} (Fig. 3), corresponding to the stretching of OH/H_2O groups. It suggests that the OH groups contained in Rutin extract become the primary substances participating in Au ion reduction. The bands detected at 2080 and 1638 cm^{-1} were attributed to the C≡C stretching of the alkyne group and amide group N–H stretching, respectively. The rutin's IR spectrum displays a band at 1654 cm^{-1} that shifted to 1638 cm^{-1} upon coordination with the Au ion. This is also considered a significant spectral shift that indicates the involvement of C=O in chelation with the Au ion. Furthermore, the peaks located at 1350 cm^{-1} and both 1180 and 1050 cm^{-1} in Rutin extract related to O–H bending and C–O stretching, respectively. Moreover, the Au–O stretching vibration band is related to the 640 cm^{-1} absorption band.

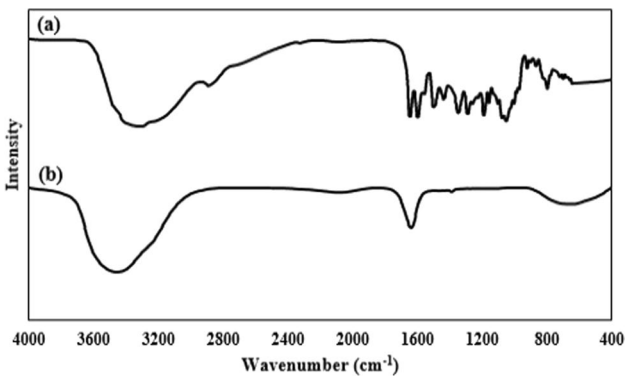

Fig. 3 FTIR spectroscopy of **a** Rutin extract and **b** Ru-Au NPs

4 Cytotoxicity of Ru-Au nanoparticles

4.1 Photothermal treatment of MCF-7 breast cancer cells

The MCF-7 live cells' number was counted by the Inverted Stage Microscope after 24, 48, and 72 h in all groups (G1–G4) (Fig. 4). The G4 (control group) revealed the cell growth's normal rate after 24 h; nevertheless, the higher MCF-7 cell count was detected from the baseline in the G4 after 48 and 72 h, which resulted from cancer cell growth and mitosis.

The other three groups (G1, G2, and G3) revealed considerably more cancer cell reduction compared with the G4 after 24, 48, and 72 h (Fig. 4). Nevertheless, G2 indicated more cancer cell destruction in comparation with G3 and G1 after 24 h, which confirms the remarkable effect of Ru-Au NPs mediated laser radiation in decreasing cancer cells compared with each treatment alone.

In recent years, laser photothermal therapy using Au NPs has attracted significant attention as a novel therapeutic method for cancer because of its potential to obtain a thermal effect on tumor tissue with minimal energy absorption and tissue destruction in surrounding tissue.

The plasmonic gold nanoparticles' efficacy for the thermo-ablation of different types of cancer cells has been investigated in some research [19]. The hyperthermia effect of laser therapy in the presence of Au NPs can damage cancer cells' DNA or vital cytoplasmic enzymes that result in cancer cell apoptosis.

Some important factors play a role in the outcomes of nanoparticle mediated laser photothermal therapy, such as the size of the nanoparticles and the wavelength of the maximal absorption [11]. Nanoparticles should have uniform size and appropriate shape with excellent dispersibility in aqueous solutions [33, 43]. They should have the ability to respond to laser light with photostability properties to support sufficient depth of penetration and photothermal effect and adequate diffusion time in the tumor environment as well as prevention of damage to surrounding healthy cells [1]. It has been revealed that different forms of gold nanoparticles (nanoshells, nanospheres, or nanorods) have the ability to get high absorptivity energy at the specific laser wavelength [44–46]. Consequently, different configurations of gold nanoparticles have been employed to improve their photothermal therapeutic properties [47, 48].

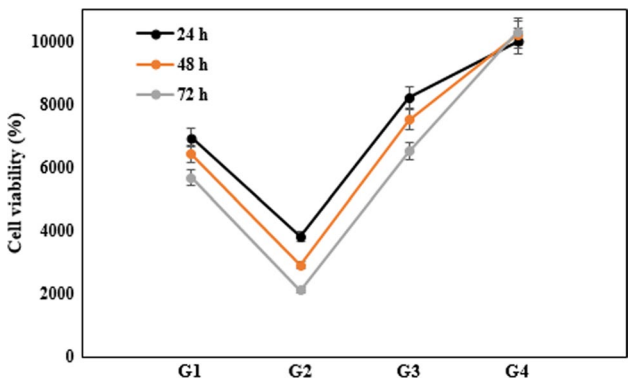

Fig. 4 The number of counted MCF-7 live cells after 24, 48, and 72 h in all groups (G1–G4)

The results of the study revealed that Ru green synthesized Au NPs in combination with laser therapy have effective and considerable PTT anticancer function on MCF-7 cells. It is suggested that the controlled ROS production in cancer cells play major role in the PTT results of Ru-Au NPS. The previous research proved the effective antioxidant characteristics and ROS production of green synthesized Au NPs [24] that inhibit susceptible cells from the progression to cancerous cells through the controlled ROS production. However, the selective targeting characteristic of rutinium through interrupting in cancer cells lipid peroxidation, can shift the lipid oxidation cycle to other accessory Pathways and produce more ROS products in cancerous cells [49]. Previous studies have reported that ROS free radicals are significantly formed within the irradiated cells that play an essential role in photodynamic therapy (PDT) results. The stress of photothermal heating by the light energy of an appropriate wavelength could produce significant amount of ROS that result in cancer cell death through the apoptosis induction or interfere in the plasma membrane integrity [50, 51].

The morphologic shape and size characteristics of green synthesized Au NPs could play substantial role in desirable results of PTT. Outcomes of Ru-Au NPs TEM images (Fig. 2) showed a uniform distribution of particle size around 40 nm and a spherical morphology that seems to induce effective plasmonic resonance properties for PTT on MCF-7 cancer cells while treated with laser therapy. Khlebtsov et al. detected that spherical shape Au NPs with 30–40 nm diameters have maximal light absorption to induce thermal effect and cancer cell death [52].

However, there are still some challenges related to plasmonic PTT mediated by Au NPs, such as limited tissue penetration's depth [53] or the unwanted toxic effect on normal cells.

The results of the MTT assay were matched with the results of counted MCF-7 live cells by an inverted stage microscope that confirmed the significant effect of laser irradiation mediated by Ru-Au NPs on cancer cell reduction (Fig. 5). Interestingly, we detected that PTT mediated by Ru-Au NPs exhibits significantly lower toxicity for normal cells than MCF-7 cells that provide the satisfactory cell safety for normal cells.

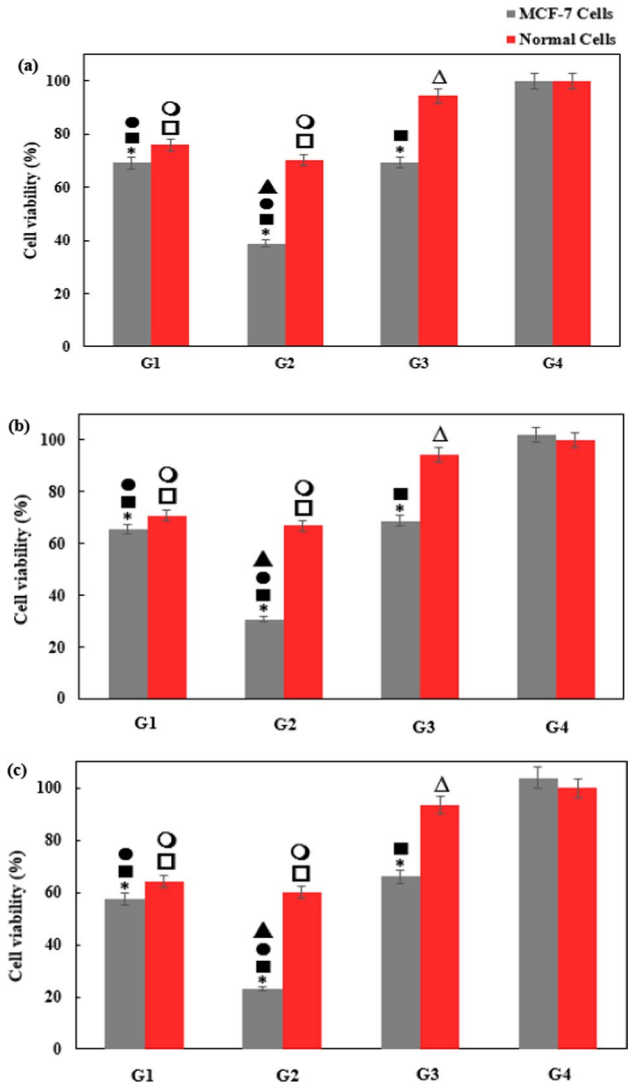

Fig. 5 Measured viability of normal and MCF-7 cells after 24, 48, and 72 h in all groups (G1-G4) by MTT. (*) *p* value significant of MCF-7 cells versus the normal cells in each group, (n) *p*-value significant of MCF-7 cells versus the control group, (o) *p*-value significant of normal cells versus the control group, (l) *p*-value significant of MCF-7 cells versus group 3, (m) *p*-value significant of normal cells versus group 3, (p) *p*-value significant of MCF-7 cells versus group 1, and (Δ) *p*-value significant of normal cells versus group 1

The results of some previous studies also detected the approximately similar cell viability and cytotoxicity of green synthesized gold nanoparticles mediated laser PTT in specific wave lengths for normal cells. However, the cell viability is closely dependent on dose and time of exposure [54–56].

The findings suggest the ability of Ru-Au NPs to produce controlled plasmon-mediated ROS products can damage cancer cells and make them vulnerable to photothermal damage, as well as the protective role of Ru-Au NPs from excessive ROS formation in normal cells, that reduce the risk of undesired side effects [24, 50].

However, to improve the PPTT results for cancer cells and decrease the cytotoxicity, it is suggested to add targeted antibodies against selected tumor tissue.

Recent developments in the Au NPs' design have enabled the generation of selectively targeted agents for PTT. For example, the capability to bind amine and thiol groups, as well as SPR, has been applied for targeted cancer therapies [57].

Selective targeted PPT can be achieved by the addition of selective antibodies against tumor specific cell components or antigens (such as transferrin or growth factors) on the Au NP surface [58]. In the study, citrate-coated Au NPs combined with anti-EGF receptor antibodies (trastuzumab) applied for the human breast cancer cells' treatment resulted in a significant decrease in cytotoxicity [59]. Kim et al. developed gold nanoparticles as an image targeting agent and subsequent targeted PTT due to their photothermal and photoacoustic characteristics [60].

Escape from the host immune system play the important role in tumor progression and metastasis [61]. Developing new techniques to boost the capability of the immune system to detect cancer cells is one of the important points in advancing targeted tumor treatment. Gold nanoparticles have been applied in this term to improve host T cell lymphocytes function to kill cancer cells.

The cytotoxic effects of biosynthetic Ru-Au NPs at 8 different concentrations of 0.25, 0.5, 1, 1.25, 1.5, 1.75, 2, and 2.5 µg/ml against normal fibroblast cells and MCF-7 cancer cells after 24, 48, and 72 h of incubation were tested by the MTT assay (Fig. 6).

The results of the MTT assay revealed that synthesized Ru-Au NPs have an effective anticancer function against MCF-7 cell lines, even in the absence of the thermal effect. This effect is more prominent in concentrations equal to or more than 0.25 µg/ml. Furthermore, there was a 30% reduction in MCF-7 cell viability at the concentration of 0.25 µg/ml Ru-Au NPs compared to the control group and increased to 70% at the concentration of 2.50 µg/ml. Outcoming data suggested that the Ru-Au NPs at concentrations of 1-2 µg/ml caused nearly 50% MCF-7 cell death.

Comparing the results with other studies, revealed that Ru-Au NPs demonstrate effective anticancer functions in lower concentrations of nanoparticles than the traditional Au NPs, even in the absence of the thermal effect. The results of MTT assay confirmed more than 50% MCF-7 cell decrease at concentration of 1.75 and 1.50 after 24 and 48 h, respectively. In a study by Nouf Omar et al. detected that less than 50% cell viability was detected at concentration of 5 µg/ml Au NPs [62]. However, various studies reported different concentrations of gold nanoparticles effective against MCF-7 breast cancer. Overall, the results obtained from

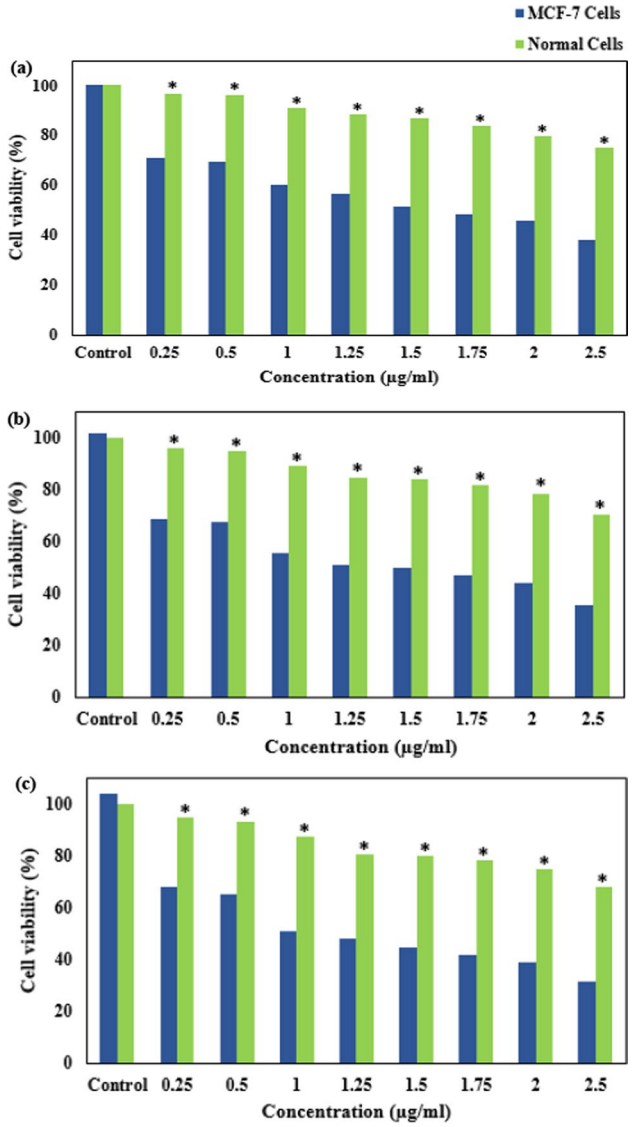

Fig. 6 Cytotoxic effects of synthesized Ru-Au NPs on normal and MCF-7 cells following exposure to different concentrations (.25, .5, 1, 1.25, 1.5, 1.75, 2, and 2.5 µg/ml) at 24, 48, and 72 hours after treating. (*) *p*-value significant of normal cells versus MCF-7 cells

different studies proved the efficient anticancer activity of Au NP's on MCF-7 breast cancer cells from the minimum concentrations of 2 µg/ml, and as the concentration increased the anticancer efficacy increased [63, 64].

As shown in Fig. 6 and in consistent with other studies, we detected a dose- and time-dependent manner of green synthesized Au NPs against MCF-7 cancer cells [65, 66]. It is suggested that the addition of Rutinium extract in Ru-Au NPs could improve anticancer properties of Au NPs through different mechanisms.

Deepika et al. revealed that Ru can inhibit cancer cells proliferation through cell cycle disruption and apoptotic induction [67]. The *p*53 gene mutation is one of the most common genetic irregularities in human tumors. Rutin can stimulate expression of the *p*53 gene activity as apoptotic gene [68, 69]. Also, it was reported that Ru could decrease Bcl-2 antiapoptosis gene expression through the reduction in the levels of MYCN mRNA [70]. It also can reduced mitochondrial membrane potential leading to mitochondrial destruction in cancer cells [71].

Previous studies have detected that green synthesized gold nanoparticles reveal better anticancer function against MCF-7 cells through long chain DNA damage or defects in cell permeability through impairment in membrane charge and integrity [72].

Also, the green synthesized Au NPs can target cancer cells' nuclei and induce cytokinesis arrest, leading to cancer cell apoptosis. However, accumulated Au NPs in the cell cytoplasm can interfere with cellular enzymes and function [73].

Consistent with our study, some previous research has also detected the considerable anticancer function of green synthesized Au NPs. In the study by Lee et al., Au NPs were functionalized in conjugation with the active flavonoid, baicalin (*Scutellaria baicalensis)*. The gold particles synthesized by baicalin revealed effective anticancer properties against the MCF-7 cell line [74]. In another study, carotenoid components of saffron stigma were applied for green synthesis of Au NPs. Au NPs conjugated with croin effectively inhibited breast cancer cell progression in a dose-dependent manner with low toxicity for normal cells [65].

Interestingly, we detected that Ru-Au NPs revealed significantly lower cytotoxicity for normal cells in comparison with MCF-7 cells (Fig. 6). It is suggested that the addition of Rutin extract to the gold nanoparticles could induce better selective targeting for MCF-7 cells or enhance its penetration into cancer cells rather than normal cells. It has been demonstrated that Ru extract can reduce the expression of miR-22-5p as target genes of microRNA in cancer cells. Subsequently the increasing levels of signaling pathway-related proteins in cancer cell cytoplasm can lead to apoptosis [75].

Previous studies have shown that Ru, can play role as antioxidant agent against lipid peroxidative products for selective targeted inhibition of cancer cell proliferation. Accumulation of pathologic components derived from accessory pathways of lipid peroxidation cycle in cancer cells can finally leads to cancer cell apoptosis [49, 76].

There are still controversies about the safety of Au NPs for normal cells. For example, some previous research has shown that Au NPs are biocompatible with less cytotoxicity for normal cells [77, 78]. However, other research has demonstrated the partial cytotoxicity of Au NPs via the production of cellular reactive oxygen species (ROS) in cytoplasm or mitochondria that results in cellular

apoptosis, especially in the reticuloendothelial system such as the spleen or liver [79, 80].

In fact, Au NPs toxicity significantly depends on their specific characteristics such as shape, size, and charge that influence NPs clearance. As expected in a physiologic condition of the human body, gold NPs with smaller sizes and coated particles usually reveal better distribution and can be rapidly excreted through the glomerular kidney system; however, larger Au NPs are more likely to accumulate in the body because of low filtration [78, 80–82].

In accordance with some other in vitro studies it was detected the effective PTT function of green synthesized Au NPs in 532 nm wavelength of light energy [83–85]. However, several parameters can limit the clinical application of Gold nanoparticles mediated photothermal therapy in in-vivo conditions, including inadequate and tissue penetration that could potentially decrease the clinical outcomes of PTT. Another parameter that could limit the clinical application of Gold nanoparticles mediated PTT is the patient's pain sensation during the treatment [86]. In addition, the long-term biocompatibility of Au NPs is not completely understood while the accumulation of Au NPs and related cytotoxicity in repetitive sessions of PTT is still unknown [87].

5 Conclusions

We report a green synthesis process to obtain a type of Au NP using Rutin as a reducing agent. The obtained Ru-Au NPs have a maximum absorption at 520–540 nm, which relates directly to the formation of a plasmonic band of Ru-Au NPs and the spherical shape with the average size of 40 nm based on TEM result. There was a statistically significant decline in MCF-7 cellular viability starting with the 0.25 µg/ml of Ru-Au NPs with acceptable safety for normal cells at these concentrations. The results indicate selective and effective anticancer function of Ru-Au NPs in addition to low cytotoxicity and better biocompatibility for normal cells. Generally, the results of this study demonstrate the prominent function and efficacy of Ru-Au NPs coupled with laser radiation (150 J/cm^2 of laser energy for 300 s) in the treatment of breast cancer MCF-7 cells compared with previous traditional Au NPs mediated PTT results. However, to improve the selectivity of the NPs for cancer cells and decreasing the side effects for normal cells, it is recommended to functionalizing nanoparticles with antibodies (Ab) targeted for breast cancer cell. As a result of the study, an ecoenvironmental nanoplatform for PPTT against MCF-7 human breast cancer cell lines with excellent anticancer function and acceptable biocompatibility has been developed.

Supplementary Information The online version contains supplementary material available at https://doi.org/10.1007/s00339-023-06832-6.

Author contributions Methodology, data analysis, and investigation: LS, HK, FSD, and MS. Data analysis, investigation, and writing–original draft, reviewing and editing: SRK. Writing, data analysis, and reviewing and editing: MA and TF. Investigation and reviewing and editing: SC. Investigation, writing, reviewing and editing, and supervision: AMA, SM-S, AV, and HK.

Data availability All data generated or analyzed during this study are included in this published article and its supplementary material files.

Declarations

Conflict of interest The authors declare that there is no conflict of interest regarding the publication of this article.

References

1. R.D. Issels, L.H. Lindner, J. Verweij, P. Wust, P. Reichardt, B.-C. Schem, S. Abdel-Rahman, S. Daugaard, C. Salat, C.-M. Wendtner, Lancet Oncol. **11**(6), 561 (2010)
2. L. Benov, Med. Princ. Pract. **24**(Suppl. 1), 14 (2015)
3. Y. Yang, Y. Hu, H. Du, L. Ren, H. Wang, Int. J. Nanomed. **13**, 2065 (2018)
4. A.H. Meisami, M. Abbasi, S. Mosleh-Shirazi, A. Azari, A.M. Amani, A. Vaez, A. Golchin, Eur. J. Pharmacol. **926**, 175011 (2022)
5. S. Mosleh-Shirazi, S.R. Kasaee, F. Dehghani, H. Kamyab, I. Kirpichnikova, S. Chelliapan, T. Firuzyar, M. Akhtari, A.M. Amani, Ceram. Int. **49**, 11293–11301 (2022)
6. C. Dennis, A. Jackson, J. Borchers, R. Ivkov, A. Foreman, P. Hoopes, R. Strawbridge, Z. Pierce, E. Goerntiz, J. Lau, J. Phys. D Appl. Phys. **41**(13), 134020 (2008)
7. Z. Starowicz, R. Wojnarowska-Nowak, P. Ozga, E. Sheregii, Colloid Polym. Sci. **296**(6), 1029 (2018)
8. S.R. Panikkanvalappil, N. Hooshmand, M.A. El-Sayed, Bioconjug. Chem. **28**(9), 2452 (2017)
9. S.K. Ghosh, T. Pal, Chem. Rev. **107**(11), 4797 (2007)
10. S. Eustis, M.A. El-Sayed, Chem. Soc. Rev. **35**(3), 209 (2006)
11. L.C. Kennedy, L.R. Bickford, N.A. Lewinski, A.J. Coughlin, Y. Hu, E.S. Day, J.L. West, R.A. Drezek, Small **7**(2), 169 (2011)
12. V.P. Torchilin, Pept. Sci. **90**(5), 604 (2008)
13. J. Chen, C. Glaus, R. Laforest, Q. Zhang, M. Yang, M. Gidding, M.J. Welch, Y. Xia, Small **6**(7), 811 (2010)
14. D.A. Giljohann, D.S. Seferos, W.L. Daniel, M.D. Massich, P.C. Patel, C.A. Mirkin, Angew. Chem. **49**(19), 3280 (2010)
15. E.B. Dickerson, E.C. Dreaden, X. Huang, I.H. El-Sayed, H. Chu, S. Pushpanketh, J.F. McDonald, M.A. El-Sayed, Cancer Lett. **269**(1), 57 (2008)
16. S. Krishnan, P. Diagaradjane, S.H. Cho, Int. J. Hyperth. **26**(8), 775 (2010)
17. A.M. Elliott, A.M. Shetty, J. Wang, J.D. Hazle, R.J. Jason-Stafford, Int. J. Hyperth **26**(5), 434 (2010)
18. A.C.P. Lage, L.O. Ladeira, L. Mosqueira, R.M. Paniago, R.O. Castilho, J.M. Amorim, E.S. Pessoa, J. Nuncira, A.A.G. Faraco, Environ. Nanotechnol. Monit. Manag. **16**, 100473 (2021)
19. C.M. Pitsillides, E.K. Joe, X. Wei, R.R. Anderson, C.P. Lin, Biophys. J. **84**(6), 4023 (2003)
20. M. Everts, V. Saini, J.L. Leddon, R.J. Kok, M. Stoff-Khalili, M.A. Preuss, C.L. Millican, G. Perkins, J.M. Brown, H. Bagaria, Nano Lett. **6**(4), 587 (2006)

21. D. Menon, A. Basanth, A. Retnakumari, K. Manzoor, S.V. Nair, J. Biomed. Nanotechnol. **8**(6), 901 (2012)
22. D.A. Selvan, D. Mahendiran, R.S. Kumar, A.K. Rahiman, J. Photochem. Photobiol., B **180**, 243 (2018)
23. A.K. Mittal, Y. Chisti, U.C. Banerjee, Biotechnol. Adv. **31**(2), 346 (2013)
24. F. Dehghani, S. Mosleh-Shirazi, M. Shafiee, S.R. Kasaee, A.M. Amani, Appl. Nanosci. **13**, 1–11 (2022)
25. S.A. Parray, J. Bhat, G. Ahmad, N. Jahan, G. Sofi, M. Ifs, Am. J. Pharm. Tech. Res. **2**(2), 239 (2012)
26. N. Saifulah, R.A. Siddiqui, M.O. Ismail, Z. Memon, Z. Aslam, M.R. Shah, Pak. J. Pharm. Sci. **33**(4), 1823 (2020)
27. A. Gul, B. Kunwar, M. Mazhar, S. Faizi, D. Ahmed, M.R. Shah, S.U. Simjee, Int. Immunopharmacol. **59**, 310 (2018)
28. K.M. Soto, I. Luzardo-Ocampo, J.M. López-Romero, S. Mendoza, G. Loarca-Piña, E.M. Rivera-Muñoz, A. Manzano-Ramírez, Pharmaceutics **14**(10), 2069 (2022)
29. K.H. Janbaz, S.A. Saeed, A.H. Gilani, Fitoterapia **73**(7–8), 557 (2002)
30. S.A. Aherne, N.M. O'Brien, Free Radical Biol. Med. **29**(6), 507 (2000)
31. M. Abbasi, R. Gholizadeh, S.R. Kasaee, A. Vaez, S. Chelliapan, F. Fadhil Al-Qaim, I.F. Deyab, M. Shafiee, Z. Zareshahrabadi, A.M. Amani, S. Mosleh-Shirazi, H. Kamyab, Scientific Reports 13(1), 5987 (2023).
32. S. Mosleh-Shirazi, M.A.J. Kouhbanani, N. Beheshtkhoo, S.R. Kasaee, A. Jangjou, P. Izadpanah, A.M. Amani, Appl. Phys. A **127**, 1 (2021)
33. S.M. Mousavi, S.A. Hashemi, A.M. Amani, H. Saed, S. Jahandideh, F. Mojoudi, Polym. Renew. Resour. **8**(4), 177 (2017)
34. S. Rostamizadeh, R. Aryan, H.R. Ghaieni, A.M. Amani, Monatshefte für Chemie-Chem. Monthly **139**(10), 1241 (2008)
35. M. Mousavi, A. Hashemi, O. Arjmand, A.M. Amani, A. Babapoor, M.A. Fateh, H. Fateh, F. Mojoudi, H. Esmaeili, S. Jahandideh, Acta Chim. Slov. **65**(4), 882 (2018)
36. H.B. Jeon, P.V. Tsalu, J.W. Ha, Sci. Rep. **9**(1), 1 (2019)
37. X. Zhong, Y.-Q. Chai, R. Yuan, Talanta **128**, 9 (2018)
38. D. Philip, Spectrochim. Acta Part A Mol. Biomol. Spectrosc. **73**(4), 650 (2009)
39. J. Kasthuri, S. Veerapandian, N. Rajendiran, Colloids Surf., B **68**(1), 55 (2009)
40. D. Philip, Spectrochim. Acta Part A Mol. Biomol. Spectrosc. **77**(4), 807 (2010)
41. S. Smitha, D. Philip, K. Gopchandran, Spectrochim. Acta Part A Mol. Biomol. Spectrosc. **74**(3), 735 (2009)
42. S. Ghosh, S. Patil, M. Ahire, R. Kitture, D.D. Gurav, A.M. Jabgunde, S. Kale, K. Pardesi, V. Shinde, J. Bellare, J. Nanobiotechnol. **10**(1), 1 (2012)
43. M. Monfared, S. Taghizadeh, A. Zare-Hoseinabadi, S.M. Mousavi, S.A. Hashemi, S. Ranjbar, A.M. Amani, Drug Metab. Rev. **51**(4), 589 (2019)
44. C. Loo, A. Lowery, N. Halas, J. West, R. Drezek, Nano Lett. **5**(4), 709 (2005)
45. M.P. Melancon, W. Lu, Z. Yang, R. Zhang, Z. Cheng, A.M. Elliot, J. Stafford, T. Olson, J.Z. Zhang, C. Li, Mol. Cancer Ther. **7**(6), 1730 (2008)
46. S.E. Skrabalak, J. Chen, Y. Sun, X. Lu, L. Au, C.M. Cobley, Y. Xia, Acc. Chem. Res. **41**(12), 1587 (2008)
47. M. Vats, S.K. Mishra, M.S. Baghini, D.S. Chauhan, R. Srivastava, A. De, Int. J. Mol. Sci. **18**(5), 924 (2017)
48. C. Loo, A. Lin, L. Hirsch, M.-H. Lee, J. Barton, N. Halas, J. West, R. Drezek, Technol. Cancer Res. Treat. **3**(1), 33 (2004)
49. E. Agmon, J. Solon, P. Bassereau, B.R. Stockwell, Sci. Rep. **8**(1), 5155 (2018)
50. V. Guerrero-Florez, S.C. Mendez-Sanchez, O.A. Patrón-Soberano, V. Rodríguez-González, D. Blach, F. Martínez, J. Mater. Chem. B **8**(14), 2862 (2020)
51. R. Vankayala, A. Sagadevan, P. Vijayaraghavan, C.L. Kuo, K.C. Hwang, Angew. Chem. Int. Ed. **50**(45), 10640 (2011)
52. B. Khlebtsov, V. Zharov, A. Melnikov, V. Tuchin, N. Khlebtsov, Nanotechnology **17**(20), 5167 (2006)
53. B.C. Wilson, M.S. Patterson, Phys. Med. Biol. **53**(9), R61 (2008)
54. A.H. Faid, S.A. Shouman, N.A. Thabet, Y.A. Badr, M.A. Sliem, J. Pharm. Innov. **18**, 144–148 (2022)
55. A. Rezaeian, S.M. Amini, M.R.H. Najafabadi, Z.J. Farsangi, H. Samadian, Lasers Med. Sci. **37**(2), 1333 (2022)
56. R.S. Riley, E.S. Day, Wiley Interdiscip. Rev. Nanomed. Nanobiotechnol. **9**(4), e1449 (2017)
57. S. Jain, D. Hirst, J. O'Sullivan, Br. J. Radiol. **85**(1010), 101 (2012)
58. M. Eghtedari, A.V. Liopo, J.A. Copland, A.A. Oraevsky, M. Motamedi, Nano Lett. **9**(1), 287 (2009)
59. W. Jiang, B. Kim, J.T. Rutka, W.C. Chan, Nat. Nanotechnol. **3**(3), 145 (2008)
60. S.-E. Kim, B.-R. Lee, H. Lee, S.D. Jo, H. Kim, Y.-Y. Won, J. Lee, Sci. Rep. **7**(1), 1 (2017)
61. R. Kim, M. Emi, K. Tanabe, Immunology **119**(2), 254 (2006)
62. N.O. Alafaleq, A. Alomari, M.S. Khan, G.M. Shaik, A. Hussain, F. Ahmed, I. Hassan, I.M. Alhazza, M.S. Alokail, A.M.H. Alenad, Nanotechnol. Rev. **11**(1), 3292 (2022)
63. W. Cai, T. Gao, H. Hong, J. Sun, Nanotechnol. Sci. Appl. **1**(2008), 17 (2022)
64. M. Kamala-Priya, P.R. Iyer, Appl. Nanosci. **5**(4), 443 (2015)
65. R. Hoshyar, G.R. Khayati, M. Poorgholami, M. Kaykhaii, J. Photochem. Photobiol., B **159**, 237 (2016)
66. S. Li, F.A. Al-Misned, H.A. El-Serehy, L. Yang, Arab. J. Chem. **14**(2), 102931 (2021)
67. M.S. Deepika, R. Thangam, T.S. Sheena, R. Vimala, S. Sivasubramanian, K. Jeganathan, R. Thirumurugan, Mater. Sci. Eng., C **103**, 109716 (2019)
68. A. Satari, S.A. Amini, E. Raeisi, Y. Lemoigne, E. Heidarian, Adv. Pharm. Bull. **9**(3), 462 (2019)
69. S. Karakurt, Acta Pharm. **66**(4), 491 (2016)
70. W. Chen, Y. Liu, M. Li, J. Mao, L. Zhang, R. Huang, X. Jin, L. Ye, J. Pharmacol. Sci. **127**(3), 332 (2015)
71. T. Kowalczyk, P. Sitarek, E. Skała, M. Toma, M. Wielanek, D. Pytel, J. Wieczfińska, J. Szemraj, T. Śliwiński, Cytotechnology **71**, 165 (2019)
72. J. Feng, L. Chen, Y. Xia, J. Xing, Z. Li, Q. Qian, Y. Wang, A. Wu, L. Zeng, Y. Zhou, ACS Biomater. Sci. Eng. **3**(4), 608 (2017)
73. B. Kang, M.A. Mackey, M.A. El-Sayed, J. Am. Chem. Soc. **132**(5), 1517 (2010)
74. D. Lee, W.-K. Ko, D.-S. Hwang, D.N. Heo, S.J. Lee, M. Heo, K.-S. Lee, J.-Y. Ahn, J. Jo, I.K. Kwon, Nanoscale Res. Lett. **11**(1), 1 (2016)
75. X. Li, Z. Liu, Y. Gu, Z. Lv, Y. Chen, H. Gao, Biomed. Res. **28**(5), 2344 (2017)
76. A. Satari, S. Ghasemi, S. Habtemariam, S. Asgharian, Z. Lorigooini, Evid.-Based Complement. Altern. Med. **2021**, 1 (2021)
77. S. Mosleh-Shirazi, M. Abbasi, M. Shafiee, S.R. Kasaee, A.M. Amani, Mater. Today Commun. **26**, 102064 (2021)
78. C. Alric, I. Miladi, D. Kryza, J. Taleb, F. Lux, R. Bazzi, C. Billotey, M. Janier, P. Perriat, S. Roux, Nanoscale **5**(13), 5930 (2013)
79. S.K. Balasubramanian, J. Jittiwat, J. Manikandan, C.-N. Ong, E.Y. Liya, W.-Y. Ong, Biomaterials **31**(8), 2034 (2010)
80. N. Khlebtsov, L. Dykman, Chem. Soc. Rev. **40**(3), 1647 (2011)
81. J.P.M. Almeida, A.L. Chen, A. Foster, R. Drezek, Nanomedicine **6**(5), 815 (2011)
82. E. Blanco, H. Shen, M. Ferrari, Nat. Biotechnol. **33**(9), 941 (2015)

83. K. Gopinath, S. Kumaraguru, K. Bhakyaraj, S. Mohan, K.S. Venkatesh, M. Esakkirajan, P. Kaleeswarran, N.S. Alharbi, S. Kadaikunnan, M. Govindarajan, Microb. Pathog. **101**, 1 (2016)
84. C. Balalakshmi, K. Gopinath, M. Govindarajan, R. Lokesh, A. Arumugam, N.S. Alharbi, S. Kadaikunnan, J.M. Khaled, G. Benelli, J. Photochem. Photobiol., B **173**, 598 (2017)
85. S.M. Al-Jawad, A.A. Taha, M.M. Al-Halbosiy, L.F. Al-Barram, Photodiagn. Photodyn. Ther. **21**, 201 (2018)
86. M. Salimi, S. Mosca, B. Gardner, F. Palombo, P. Matousek, N. Stone, Nanomaterials **12**(6), 922 (2022)
87. J.B. Vines, J.-H. Yoon, N.-E. Ryu, D.-J. Lim, H. Park, Front. Chem. **7**, 167 (2019)